Cement & Concrete Composites 42 (2013) 49–58

Contents lists available at SciVerse ScienceDirect

Cement & Concrete Composites

journal homepage: www.elsevier.com/locate/cemconcomp

Improved durability of vegetable fiber reinforced cement composite subject to accelerated carbonation at early age

A.E.F.S. Almeida [a,*], G.H.D. Tonoli [b], S.F. Santos [a], H. Savastano Jr. [a]

[a] *Dept. of Food Engineering, University of São Paulo (USP), Av. Duque de Caxias Norte, 225, CEP 13635-900, Pirassununga, SP, Brazil*
[b] *Dept. of Forest Science, Federal University of Lavras, P.O. Box 3037, CEP 37200-000, Lavras, MG, Brazil*

ARTICLE INFO

Article history:
Received 18 July 2012
Received in revised form 29 January 2013
Accepted 7 May 2013
Available online 16 May 2013

Keywords:
Vegetable fiber
Fiber cement composite
Microstructure
Mechanical properties
Carbonation
Cure

ABSTRACT

This work presents the improved mechanical properties of eucalyptus pulp reinforced cementitious composites produced by the slurry-dewatering and pressing technique. They were subjected to accelerated carbonation after 2 days of controlled curing, which was investigated aiming to find a durable composite with vegetable pulp as an exclusive reinforcement. The effect of carbonation curing on the mechanical, physical, and microstructural properties of composites at 28 days of age, after 200 and 400 accelerated aging cycles and one year of natural weathering was evaluated. The interaction of the reduction in $Ca(OH)_2$ content, the increase in $CaCO_3$ content, the lower porosity, the higher density and the good fiber–matrix adhesion can explain the better mechanical performance after the aging conditions, indicating the improved durability of carbonated composites.

1. Introduction

Vegetable fiber reinforced cement-based composites are increasingly used as building materials [1–4]. The cellulosic fiber addition can result in the improvement of mechanical properties and is essential in the processing of the fiber cement when the Hatschek process is applied [3]. Moreover, these fibers are derived from renewable resources and are cheaper than polymeric fibers. However, the long term durability of these air-cured composites is a problem due to the deterioration caused by several mechanisms associated with the environment (i.e. natural weathering), which have been investigated in order to mitigate the degradation [2–10]. In addition to the environmental effect, alkaline hydrolysis of cellulose molecules in the highly alkaline cementitious matrix due to the high calcium hydroxide content is an important mechanism. Chemical compositions of natural fibers (e.g. lignin) are susceptible for dissolution in this alkaline medium, resulting in a decrease in the tensile strength of these fibers [1,4].

Accelerated carbonation is a developing technology which may have potential for the treatment of wastes and contaminated soils and for the sequestration of CO_2, an important greenhouse gas. The effect of the accelerated carbonation reactions on solid phases of the different materials has been studied taking into consideration the positive results of this technique [11]. The mechanism of carbonation can be described as the diffusion of CO_2 from the atmosphere through unsaturated pores of the cementitious matrix. The CO_2 is dissolved in the aqueous phase in the pores and transformed into carbonic acid (H_2CO_3), which is dissociated in ions HCO_3^- and CO_3^-. Additionally, the calcium hydroxide ($Ca(OH)_2$) is dissolved in Ca^{2+} and OH^- ions, resulting in the precipitation of calcium carbonate ($CaCO_3$). Therefore, a minimum content of water is essential for the ionization of compounds to promote the reaction of carbonation, but a large amount of water (i.e. saturated pores) limits the reaction due to the blockage of the pores [11]. The parametric study concerning the CO_2 reaction with each compound of cement was described by Peter et al. [12].

The accelerated carbonation immediately after casting resulted in mortars with higher strength [13]. Single cement compounds submitted to accelerated carbonation immediately after mixing resulted in higher strength development of the silicate phases [14]. Tonoli et al. [8] evaluated the effect of carbonation applied at 28 days of age on the durability of cementitious composites reinforced with Kraft sisal pulps used to produce roofing tiles. They concluded that this procedure improved the mechanical strength, decreased the calcium hydroxide content and a denser matrix was reported. Experimental work showed that accelerated aging in a CO_2 environment reduced the porosity, water absorption, and nitrogen permeability in the cement matrix and enhanced the durability of vegetable fiber cement based composites [15,16].

The present study continued the previous research on advantageous curing conditions [9]. Despite the fact that research on the

---

[*] Corresponding author. Tel.: +55 19 3565 4269; fax: +55 19 35654114.
E-mail address: alessandra.efsa@gmail.com (A.E.F.S. Almeida).

0958-9465/$ - see front matter © 2013 Elsevier Ltd. All rights reserved.
http://dx.doi.org/10.1016/j.cemconcomp.2013.05.001

carbonation of cement paste, cured concrete and fiber composites is extensive, studies on the carbonation of vegetable fiber cement based composites after initial hardening (but within 50 h) followed by a successive controlled hydration are incipient. Taking into consideration the advantages of the carbonation process reported by the literature, this paper reports the improved mechanical properties of eucalyptus pulp reinforced cement based composites produced by the slurry-dewatering and pressing technique and submitted to the accelerated carbonation in the early stages of hydration. This curing condition was investigated to mitigate the cellulose fiber degradation in the cementitious composites for the maintenance of their mechanical performance under aggressive conditions.

2. Experimental

2.1. Materials

The formulation was based on previous studies carried out in an attempt to produce durable fiber cement by the slurry-dewatering technique and using vegetable pulps as reinforcement [17,18]. The following materials and ratios were used (by dry mass): 10.0% of unrefined unbleached eucalyptus cellulosic pulp, 77.2% of Portland cement type CPV-ARI [19] and 12.8% of ground carbonate material industrialized for agricultural application, which was added as partial substitution of Portland cement in order to reduce the cost. High early strength Portland cement is free from mineral additions (blast furnace slag or pozzolans) and was selected because it minimizes the influence of those additions on the carbonation mechanism. Chemical compositions (% by mass of oxides) of the cement and ground carbonate material were determined using X-ray fluorescence spectrometry and are presented in Table 1. Morphological properties of the unrefined unbleached eucalyptus pulp are presented in Table 2 [18]. Total residual lignin content (TRLC) and the amount of wood extractives of the pulp was 2.2 ± 0.1% w/w and 0.5 ± 0.1% w/w, respectively [7].

2.2. Composite preparation and curing

Fiber reinforced cement plates measuring 200 mm × 200 mm × 5 mm were cast in the laboratory as described by Tonoli et al. [17] using a slurry-dewatering process followed by a pressing technique, as an approximate reproduction of the Hatschek process applied by the industrial production of fiber cement [20]. After these steps were taken, the samples were exposed to two different curing conditions based on preliminary results:

(a) *Non-Carbonated Curing* (NCC). The samples were placed into a climatic chamber at 60 °C and 90% RH for 2 days. Following this step, the samples were maintained in air saturated curing (i.e. sealed in plastic bags) under 25 °C until they attained the age of 28 days. These samples are identified as non-carbonated composites in this work.

(b) *Accelerated Carbonation Curing* (ACC). The samples were placed in a climatic chamber at 60 °C and 90% RH for the two initial days, following the accelerated carbonation applied to the specimens by means of CO_2 cycles released into the chamber up to the total saturation of the environment. These cycles were carried out until carbonation of the samples was observed. After this, they were kept in air saturated curing (i.e. sealed in plastic bags) under 25 °C until 28 days of age. These samples are called carbonated composites.

The initial curing condition was carried out under 60 °C in order to accelerate the hydration reactions and the uptake of CO_2 which increases with temperatures of up to 60 °C [11]. The carbonation depth of the cement matrix was observed by spraying a solution of phenolphthalein onto the freshly broken surfaces, i.e. the cross-section of the samples, which is frequently used as an indicator of the pH [8,12,21]. This solution is purple when reacting with alkaline substances and is colorless in the presence of acid substances, indicating the carbonation reaction in the cement matrix due to the lower $Ca(OH)_2$ content that decreases the pH. The CO_2 cycles inside the chamber were stopped when the purple color was not observed in the whole cross-section of the sample, which occurred after three days of accelerated carbonation.

After controlled curing until the age of 28 days, the composites were exposed to accelerated aging tests and 1 year of natural weathering to evaluate their durability.

2.3. Natural and accelerated aging tests

Composite durability was estimated by means of accelerated aging tests and also by exposing the specimens to one year of natural weathering.

2.3.1. Natural weathering

Specimens were exposed to 1 year of natural weathering (1 YNW) in Pirassununga (rural environment), State of São Paulo, Brazil (21°59′S of latitude). The composites were positioned in a metallic structure facing north with a 30° slope in relation to the horizontal plane. The environmental conditions were monitored in the weather station, which recorded the data daily. For the period of exposure, the mean annual relative humidity was 84%, the mean annual temperature was 21.4 °C and the annual rainfall was 2310 mm.

2.3.2. Accelerated aging cycles

The accelerated aging test aims to speed up natural weathering in the laboratory using soaking and drying cycles. Specimens were successively immersed into water at 20 ± 5 °C for 170 min and, after an interval of 10 min, they were heated to the temperature of 70° ± 5°C for 170 min in a ventilated oven. Another interval of 10 min at room temperature also preceded the subsequent cycle, as recommended by the EN 494 Standard [22]. Each cycle finished when one soak and dry is completed and the samples were submitted to 200 accelerated aging cycles (200 AAC) and 400 accelerated aging cycles (400 AAC).

Table 1

Chemical composition of cement and ground carbonate (% by mass of oxides).

	CaO	MgO	SiO_2	Al_2O_3	Fe_2O_3	Na_2O	K_2O	SO_3	MnO	P_2O_5	TiO_2
Portland cement[a]	63.5	3.1	19.4	4.1	2.3	0.2	1.1	3.0	–	–	–
Carbonate	39.1	8.9	9.0	2.2	1.2	0.1	0.4	–	<0.1	0.2	0.1

[a] NBR 5733 [19] (clinker + gypsum = 100–95% by mass; carbonate material = 0–5%).

Table 2
Morphological properties of eucalyptus unbleached pulp[a].

Pulp CSF[b] (mL)	Length[c] (mm)	Average width (μm)	Aspect ratio	Curl (%)[d]	Fibrous material (10^6 fibres/g)	Fines content (%)[e]
664	0.83 ± 0.05	16.4 ± 0.2	51	8.6 ± 0.2	18.2 ± 1.1	8.1 ± 1.0

[a] Fibres were analyzed by a PulptecTM MFA-500 morphology fibre and shive analyzer – MorFiTrac [18].
[b] The canadian standard freeness (CSF) is a recognized standard test to determine the rate of drainage of a diluted pulp suspension.
[c] Length weighed in length.
[d] Gradual and continuous curvature of the fibres.
[e] A fine element was considered as any detected object present in the pulp with dimensions lower than those of the fibers, i.e. length under 200 μm or width under 5 μm.

2.4. Mechanical and physical tests

Mechanical and physical properties were obtained for both non-carbonated curing (NCC) and accelerated carbonation curing (ACC) composites that were evaluated in the conditions:

- At 28 days of controlled curing and therefore accelerated aging cycles were not performed. This condition was denoted as unaged.
- After 200 accelerated aging cycles (200 AAC).
- After 400 accelerated aging cycles (400 AAC).
- After 1 year of natural weathering (1 YNW).

Each fiber cement pad was wet cut into four specimens measuring 165 mm by 40 mm for the mechanical test, using a water cooled diamond saw. Mechanical tests were performed in a universal testing machine Emic DL-30.000 equipped with 1 kN load cell. A four-point bending configuration, a lower span of 135 mm, an upper span of 45 mm and a deflection rate of 1.5 mm/min were adopted in the tests to determine the limit of proportionality (LOP), the modulus of rupture (MOR), the modulus of elasticity (MOE) and specific energy (SE) of eight specimens for each condition. The deflection during the bending test was collected by the deflectometer positioned in the middle span at the bottom of the specimen. The values of deflection were divided by a span of 135 mm and called specific deflection in the present work. Mechanical properties were obtained using Eqs. (1)–(3) as described in detail by Tonoli et al. [17,23]:

$$\mathrm{MOR} = \frac{P_{\max} \cdot L_v}{b \cdot h^2} \tag{1}$$

$$\mathrm{LOP} = \frac{P_{\mathrm{lop}} \cdot L_v}{b \cdot h^2} \tag{2}$$

$$\mathrm{MOE} = \frac{276 \cdot L_v^3}{1296 \cdot b \cdot h^3} \cdot m \tag{3}$$

where $P_{\max}$ is the maximum load value, P_{lop} is the load at the upper point of the linear portion of the load–deflection curve, L_V is the major span, b and h are the specimen width and depth respectively and m is the tangent of the slope angle of the load vs. deflection plotting in the elastic behavior.

Specific energy was defined as the energy absorbed during the bending test divided by the cross-sectional area of the specimen. The absorbed energy was obtained by integrating the load vs. deflection curve up to the point which corresponds to a reduction in the load carrying a capacity of 30% of the maximum reached.

The physical properties, bulk density (BD) and apparent void volume (AVV) were obtained from an average of seven specimens for each aging condition, following procedures specified by the ASTM C 948 Standard [24].

2.5. Microstructural characterization

Mercury Intrusion Porosimetry (MIP) measurements were used to determine the pore size distribution using a Micromeritics Poresizer 9320. The parameters used were pressure up to 200 MPa, stabilization time in the low and high pressure settings was 10 s, assuming the value of surface tension of 0.485 N/m and a contact angle of 130°, which was used in the Washburn equation to convert applied pressure to pore diameter. Despite the fact that this technique loses its accuracy for “ink-bottle” pores and fractures can be possibly induced in samples under high intrusion pressure [25], the MIP measurement is the preferred method for pore structure evaluation due to its large range of pore size measurements and easy operation. In addition, MIP can be considered an acceptable tool for a comparative study of the pore-structure of cement-based materials under specific conditions. MIP was performed in this work to compare the pore structure of carbonated and non-carbonated samples.

X-ray diffraction (XRD) was used to identify the polycrystalline phases of fiber reinforced cement composites by means of the X-ray patterns that are unique for each of the crystalline phases identified by the International Centre for Diffraction Data (ICDD). The influence of the carbonation on the cement hydration was investigated by the portlandite (calcium hydroxide) content, that can be estimated by the peak intensity in the region of $2\theta = 18°$. The qualitative investigation was performed in a Rigaku Rotaflex RU 200B model with Cu Kα radiation at 2° per minute using a step size of 0.02°.

The hydration process of Portland cement can also be evaluated by measuring the weight loss of hydrated samples up to 800°C. Thermogravimetry analysis (TGA) and derivative thermogravimetry (DTG) were used for evaluating the nature of hydration products formed in cement-based systems. The different DTG peaks reported when hydrated cement is heated in the thermobalance are [21,26–31]:

- 100 °C – weight loss due to the dehydration of water pore.
- 100 °C to 300 °C – different stages of dehydration of C–S–H.
- 500 °C – dehydroxylation of $Ca(OH)_2$.
- 700 °C – decarbonation of $CaCO_3$.

The major thermal decomposition for cellulose occurs within a steep region ranging from 300 to 380 °C [29–31].

The TGA analyses were performed using TGA 2050 Thermogravimetric Analyzer equipment. The experimental conditions were: N_2 gas dynamic atmosphere ($40\ \mathrm{mL\ min^{-1}}$); heating rate ($10\ °\mathrm{C\ min^{-1}}$) and a platinum top-opened crucible. The samples were heated in the range of 20–900 °C at a constant rate. The $Ca(OH)_2$ and $CaCO_3$ were estimated from the weight loss measured in the TGA curve between the initial and final temperature of the corresponding DTG peak.

The preparation of the samples for TGA and XRD studies was carried out using an agate crucible, in which the composite was manually ground until the size of particles was smaller than

63 μm. For the prevention of carbonation and maintenance of relative humidity, all specimens were stored under vacuum up to the time in which the test started.

The effect of the early-stage accelerated carbonation curing on the fracture surfaces resulting from the mechanical tests at 28 days was analyzed by scanning electronic microscopy (SEM) using a PHILIPS XL 30 FEG microscope and a secondary electron detector.

3. Results and discussion

3.1. Mechanical and physical properties

The typical load vs. specific deflection curves showed evidence that the non-carbonated composites were severely degraded as a result of the accelerated aging cycles, indicating that there was a significant decrease in the load and strain values, as a consequence of their embrittlement (Fig. 1a). Different mechanical behavior was found for the carbonated composites after aging (Fig. 1b). The typical curves for the carbonated composites before and after aging cycles indicated a better mechanical performance. It suggests that the strength of the fiber was maintained in a less alkaline matrix and with an improved fiber–matrix transition zone, allowing the dissipation of energy in the post-cracking region.

The BD and AVV are interrelated and their values are a result of the microstructure and compounds produced in the cementitious matrix hydration. The carbonated composites showed the lowest results for AVV (Fig. 2) and the highest values of BD (Fig. 3). The carbonation reactions can fill the pores in the matrix with carbonate products, decreasing AVV and increasing BD for the reason that the $CaCO_3$ compound produced from the carbonation reaction is denser than $Ca(OH)_2$. The AVV values decreased by the carbonation cure and also after each aging condition (for the carbonated and non-carbonated samples) due to the progress of the hydration process and the natural carbonation for the natural weathering condition.

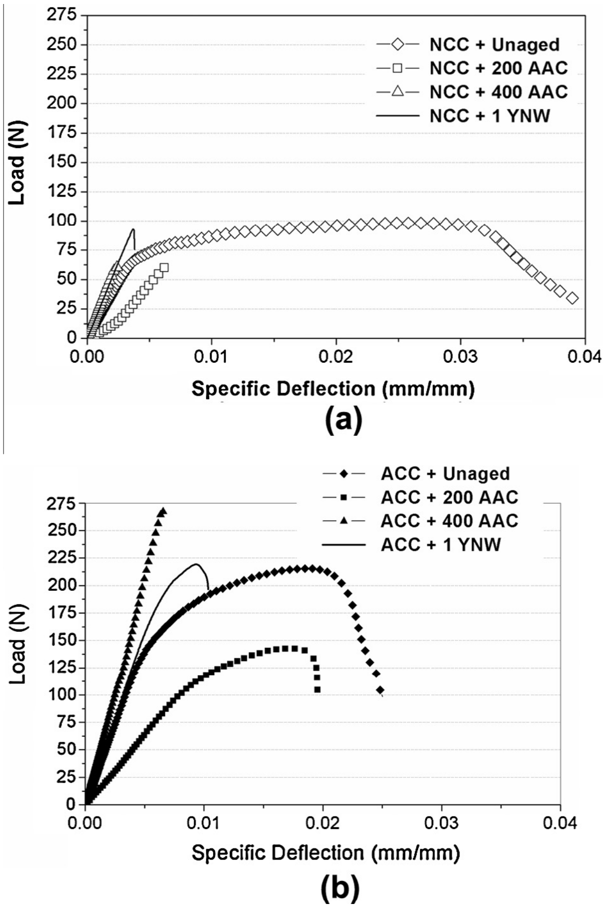

Fig. 1. Typical load vs. specific deflection curves of composites at 28 days (Unaged) and after accelerated aging cycles (AAC): (a) non-carbonated curing (NCC); and (b) accelerated carbonation curing (ACC).

Figs. 2 and 3 show the relationship between LOP, MOR, MOE, SE and physical properties. The decrease of the AVV (Fig. 2) and the increase of the BD values (Fig. 3) considerably contributed to maintaining the improved mechanical properties of the carbonated cementitious matrix. The carbonated composites showed higher average values of MOR, MOE and LOP than non-carbonated ones, taking into account results at 28 days (unaged) and after the aging conditions.

The LOP was reduced to approximately 4 MPa for the non-carbonated samples, except for the samples exposed to one year of natural weathering (Fig. 2a). The carbonated samples presented an average value equal to 13 MPa, including samples after 400 AAC.

MOR values indicate that the fibers and matrix work together after the first cracking, as a result of their effective adhesion. Fig. 2b shows that carbonated samples presented higher MOR for all aging tests (Unaged, 200 AAC, 400 AAC and 1 YNW), with an average value equal to 19 MPa. For the non-carbonated samples, the highest MOR was found for the samples exposed to one year of natural weathering due to the carbonation process with the CO_2 from the atmosphere, and the lowest is approximately 4 MPa after 400 AAC.

Tolêdo Filho et al. [10] have studied cement based specimens reinforced with sisal and coir chopped fibers with similar mechanical behavior. The strength of the aged material increased and this was attributed to the elimination of calcium hydroxide due to the carbonation treatment (109 days in a CO_2 incubator).

SE average values were higher for the carbonated samples (Fig. 3b), approximately 2 kJ/m^2 at 28 days and 1 kJ/m^2 after accelerated and natural aging in contrast with the non-carbonated ones that showed a marked decrease in this property to 0.1 kJ/m^2 after all aging conditions, indicating their embrittlement. SE values decreased slightly after aging tests for the carbonated ones suggesting that the higher bulk density by the precipitation of calcium carbonate can mitigate the effects of soaking and drying cycles, thus preserving the fiber and also the fiber matrix bonding. Therefore, a higher density due to the accelerated carbonation curing maintained the energy absorption capacity by a good fiber matrix bonding which improved the bridging effect of the fibers.

The mechanical properties were improved after 400 AAC when compared with 200 AAC results, mainly for the modulus of elasticity (Fig. 3a). Accelerated aging cycles caused a reduction in the apparent void volume content in the composites, which may be correlated with the progress of the hydration process. In addition, an increase in the $Ca(OH)_2$ content for the carbonated and non-carbonated composites after 400 AAC was observed, as reported by the thermogravimetric study (Table 3). These results show evidence of progress in the cement hydration process which can explain the results after 400 AAC.

Soroushian et al. [32] studied the effect of accelerated CO_2 curing on the structure and durability of cellulose fiber cement composite using Southern Softwood Kraft pulp. Thin-sheet cellulose fiber reinforced cement composites were manufactured using fibers, sand, a flocculating agent, silica fume and Type I Portland cement in the slurry-dewatering method, followed by pre-curing in the oven or carbonation chamber and finally the composites were autoclaved. This work found the improvement in the flexural toughness of unpressed cellulose fiber-reinforced cement composites with CO_2 curing under accelerated aging effects.

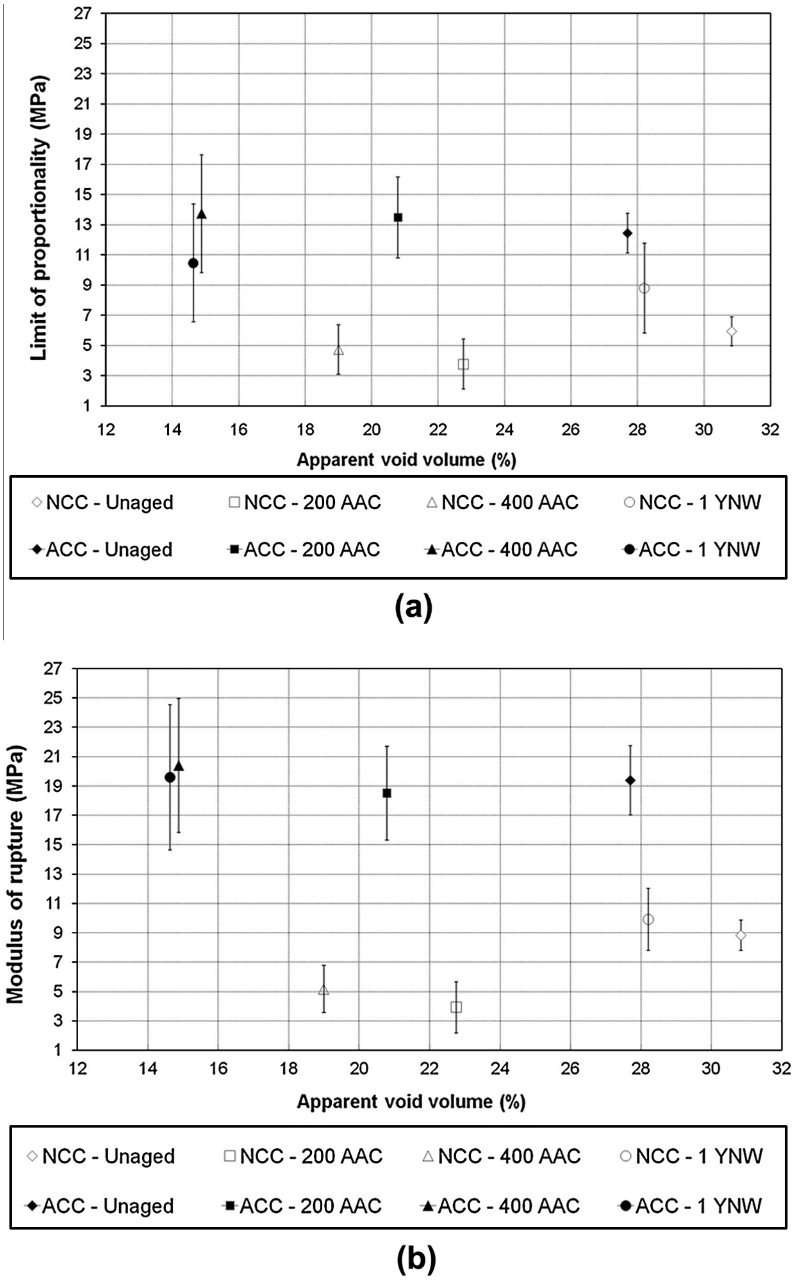

Fig. 2. Average values of mechanical properties vs. apparent void volume (AVV): (a) limit of proportionality (LOP); and (b) modulus of rupture (MOR).

3.2. Microstructural properties

A microstructural investigation intends to explain the basic mechanisms involved in the CO_2 curing process which improved the mechanical properties of the carbonated composites.

3.2.1. Mercury intrusion porosimetry

The pore size distribution and total porosity of carbonated and non-carbonated samples measured by MIP after accelerated and natural aging conditions are shown in Fig. 4. This figure shows that the pore size distribution is strongly influenced by the accelerated carbonation curing condition, which resulted in small changes after aging conditions. According to the literature, a large amount of capillary pores (which range from 0.01 μm to 10 μm) and macropores (i.e. pores larger than 0.05 μm) has an unfavorable effect on the strength and permeability properties of cement based materials as follows [33]:

- Gel pores are interconnected interstitial spaces between the gel particles in the diameter range smaller than 10 nm that influences shrinkage and creep. Pore diameters greater than 10 nm were evaluated by MIP, as shown in Fig. 4.
- Medium capillaries range from 10 to 50 nm and influence strength, permeability, creep and shrinkage. Carbonated and non-carbonated composites presented a lower volume of mercury intruded into this pore size.
- Large capillaries from 50 nm to 1 μm influence the strength and permeability. Carbonated composites presented the lowest volume of mercury intruded for this range which can clarify mechanical performance and corroborates to the lower void volume resulted in the physical test. On the other hand, non-

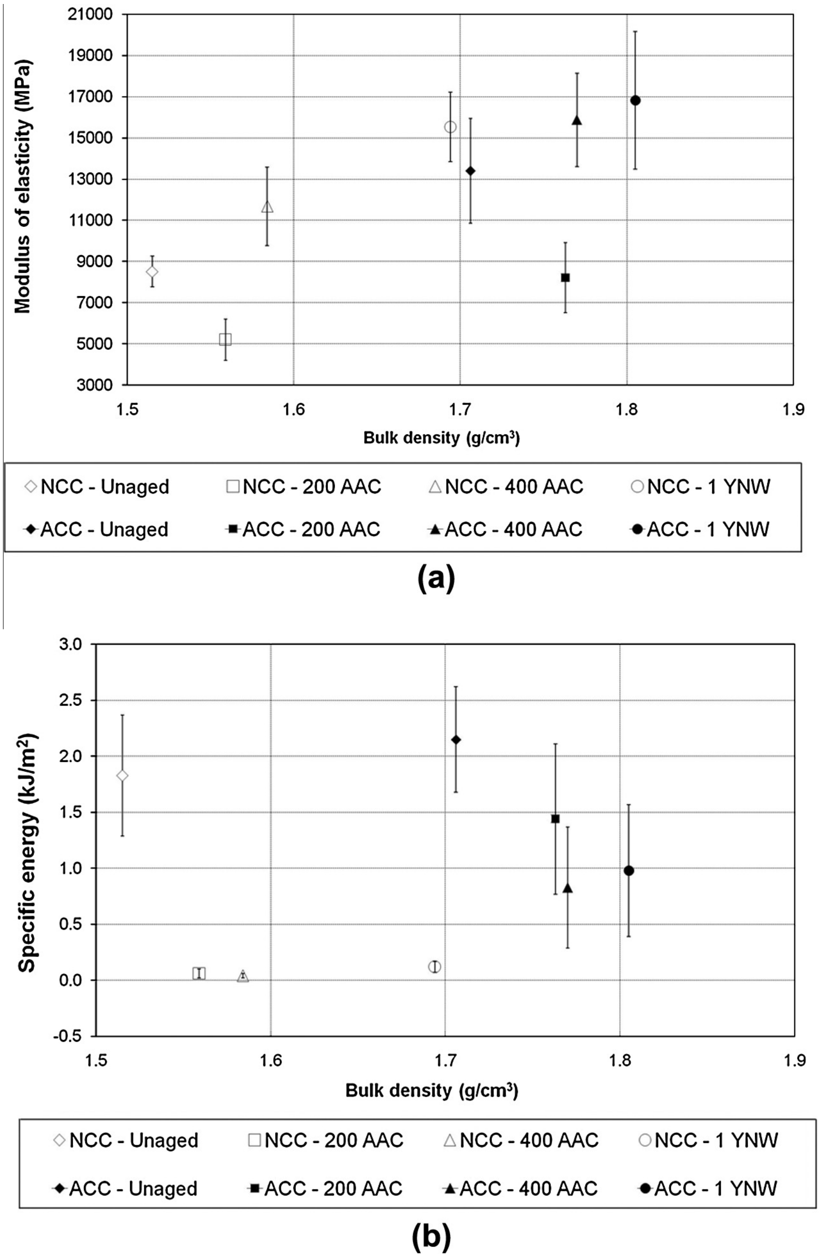

Fig. 3. Average values of mechanical properties vs. bulk density (BD): (a) modulus of elasticity (MOE) and (b) specific energy (SE).

Table 3
Calcium hydroxide and calcium carbonate content in composites.

Condition of aging	%CH_{DH-NC}[a] (Eq. (4))	%CC_{NC}[b] (Eq. (3))	%CH_{DH-C}[c] (Eq. (4))	%CC_{C}[d] (Eq. (3))
Unaged	10.3	22.7	2.9	40.1
200 AAC	10.3	22.7	2.9	40.1
400 AAC	11.5	26.1	7.4	40.1
1 Year of natural weathering	9.9	31.1	7.4	40.1

[a] %CH of non-carbonated composite.
[b] %CC of non-carbonated composite.
[c] %CH of carbonated composite.
[d] %CC of carbonated composite.

carbonated composites showed an increase in the mercury volume intruded for this range that justifies their poor mechanical performance.

- Large capillaries and entrained air are associated with a pore size larger than 1 μm and influences the strength. In this work, carbonated composites showed a considerable lower volume of mercury intruded into this pore size, contrary to non-carbonated ones that showed an appreciable volume of mercury intruded, approximately in the range of 1 μm.

As can be seen, the accelerated carbonation curing resulted in a lower pore volume in the macropore range (i.e. pores larger than 0.05 μm), which can explain their better mechanical performance after all conditions (Unaged, 200 AAC, 400 AAC and 1 YNW).

The total volume of pore space intrudable by mercury may also be useful as a comparative index of the porosity for cement based materials in a specific condition [25]. The relationship between total intrusion volume and the average pore size of composites obtained by MIP are shown in Fig. 5. It can be clearly seen that the average pore size and total intrusion volume of mercury are signif-

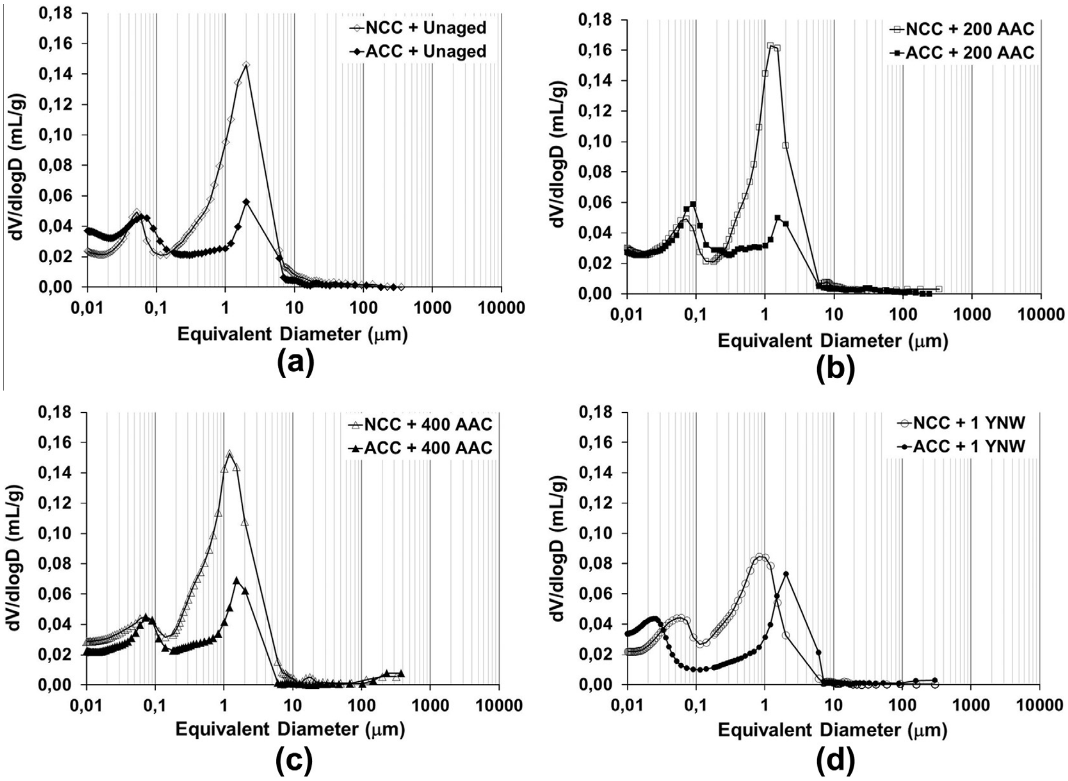

Fig. 4. Pore size distribution for non-carbonated (NCC) and carbonated composites (ACC): (a) Unaged; (b) 200 accelerated aging cycles (200 AAC); (c) 400 accelerated aging cycles (400 AAC); and (d) 1 year of natural weathering (1 YNW).

icantly decreased with the carbonation curing and maintained for all aging conditions, comparing with the non-carbonated cuing.

The accelerated aging cycles resulted in a slight decrease in the average pore size and porosity for the non-carbonated composites (Fig. 5). In addition, the average pore size and porosity were significantly reduced for non-carbonated samples after being exposed for one year of natural weathering due to natural carbonation, which occurred slowly. In natural weathering, a reduction of porosity of the composite is expected because $Ca(OH)_2$ reacts with CO_2 from the atmosphere to form $CaCO_3$, which is denser than $Ca(OH)_2$.

3.2.2. Thermogravimetric analysis

DTG curves were plotted for each TGA of the carbonated and noncarbonated composites after all aging conditions (Fig. 6). According to the literature, weight loss in the peak of 450 °C shown in the DTG curve is reported as the dehydroxylation of the calcium hydroxide and the peak of 700 °C is related to the decarbonation of calcium carbonate as shown in Eqs. (4) and (5), respectively. The thermal decomposition for cellulose and other hydrated compounds (i.e. the silicates and aluminates) can be observed in the range of 300 to 380 °C for all the samples.

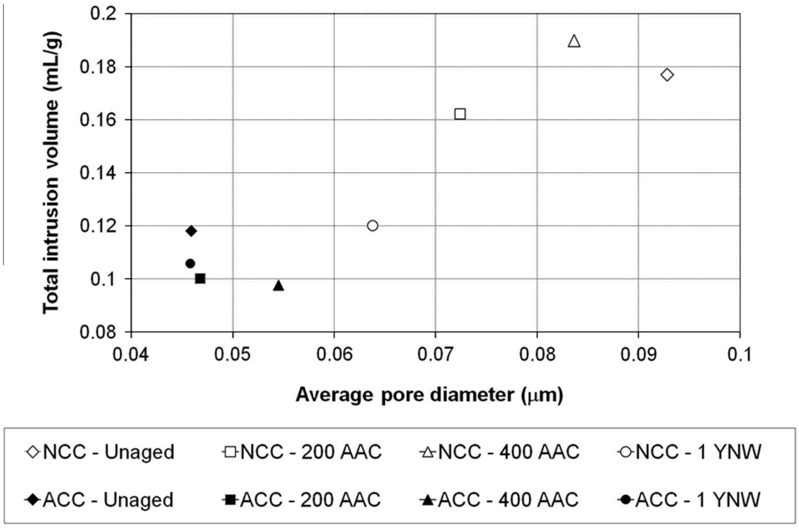

Fig. 5. Relationship between total intrusion volume and average pore diameter.

$$Ca(OH)_{2(s)} \rightarrow CaO_{(s)} + H2O_{(g)} \tag{4}$$

$$CaCO_{3(s)} \rightarrow CaO_{(s)} + CO_{2(g)} \tag{5}$$

As can be seen, non-carbonated samples presented a higher weight loss in the peak of 450 °C than carbonated ones, approximately 2.5% for unaged samples and after 200 AAC, 2.8% after 400 AAC and 2.4% after 1 YNW, due to the dehydroxylation of the $Ca(OH)_2$. For the peak at 700 °C, they presented approximately 10% for the unaged and after 200 AAC, 11.5% after 400 AAC and 13.7% after 1 YNW. The carbonated composites showed a higher weight loss for the peak of 700 °C, approximately 18% for all conditions, suggesting higher $CaCO_3$ content in the matrix as a result of the carbonation reaction, and a lower weight loss for the peak of 450 °C, approximately 0.7% for the unaged samples and after 200 AAC, and 1.8% for the samples after 400 AAC and after 1 YNW.

It was considered that CO_2 is the only gas emitted in the temperature range of 600–700 °C and that this method is not completely accurate [21]. However, it was useful for a comparative study between accelerated carbonation cured samples and non-carbonated ones in the specific conditions of this work. The amount of calcium hydroxide (CH) and calcium carbonate (CC) were estimated using the molar mass balance according to their equations, considering that 74 g/mol, 18 g/mol, 100 g/mol and 44 g/mol are the molar masses of $Ca(OH)_2$, H_2O, $CaCO_3$ and CO_2, respectively.

The amount of CC was calculated using Eq. (6) and the CO_2 loss (L_1) was obtained from TGA/DTG in the decarbonation range (approximately 700 °C) according to Eq. (5). The calcium hydroxide (CH_{DH}) was estimated from the dehydroxylation loss (L_2), as shown in Eq. (4), and calculated by Eq. (7) [21].

$$\%CC = L_1 \cdot 100/44 = 2.27 \cdot L_1 \tag{6}$$

$$\%CH_{DH} = L_2 \cdot 74/18 = 4.11 \cdot L_2 \tag{7}$$

As reported in Table 3, non-carbonated samples presented the highest $\%CH_{DH}$ for all aging conditions, i.e. 10.3% of CH was not carbonated and is responsible for the high pH at 28 days of age. This result was not observed for the carbonated samples that showed the lowest $\%CH_{DH}$ (2.9%) and therefore their pH was decreased to the acid range as detected using the phenolphthalein test. This decrease of pH should have contributed to reduce the degradation of the fibers by the higher alcalinity.

The amount of CC for carbonated samples was higher for all aging conditions (40.1%) than non-carbonated ones (22.7%), which showed CC resulting from the raw materials and the carbonation reaction in the natural weathering condition, which in turn increased the CC to 31.1%.

Table 3 shows an increase in the portlandite content for the carbonated sample after 400 AAC and a slight increase for the non-carbonated ones, as a result of the progress in the hydration process.

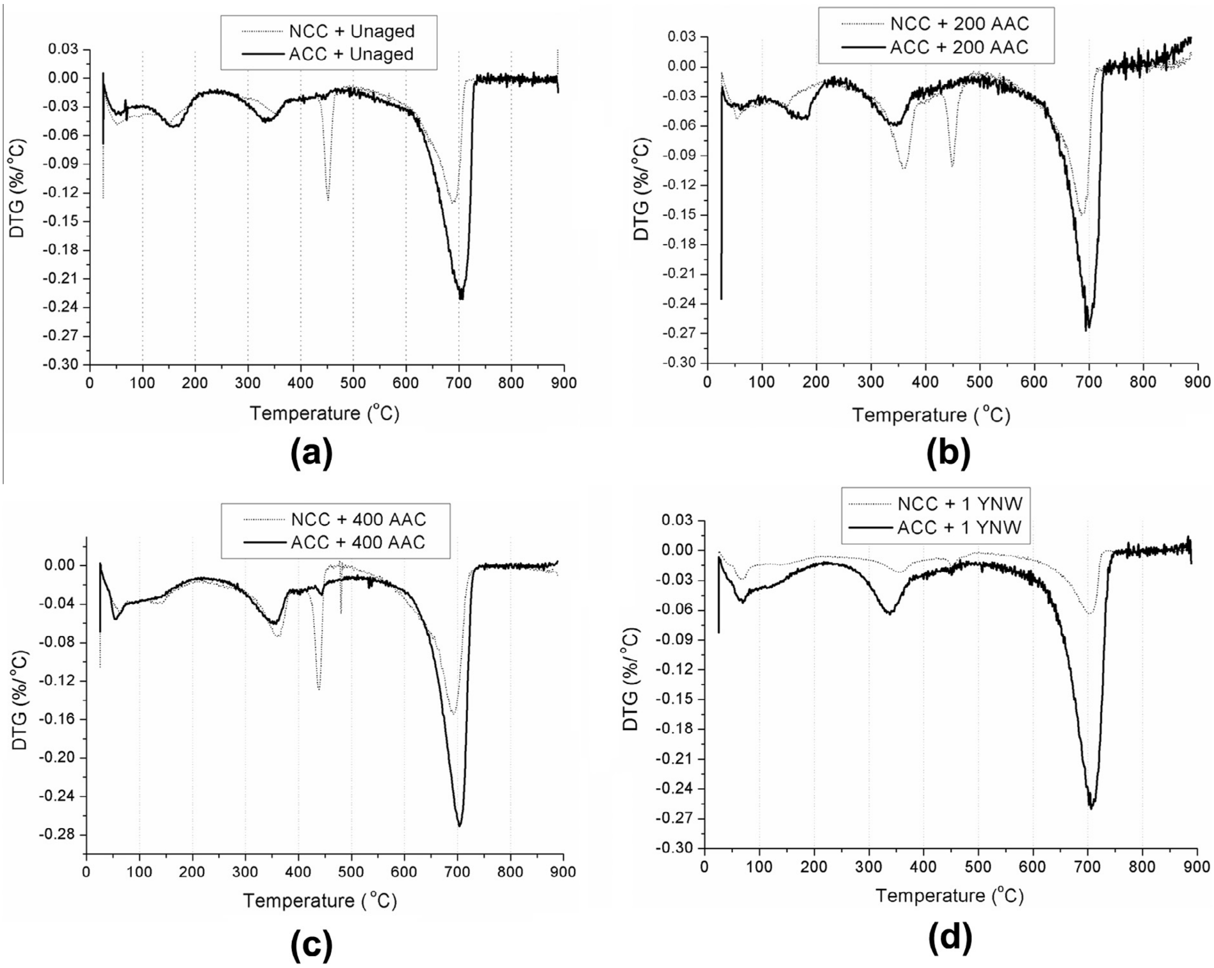

Fig. 6. DTG curves of non-carbonated (NCC) and carbonated (ACC) composites: (a) Unaged; (b) 200 AAC; (c) 400 AAC; and (d) 1 YNW.

3.2.3. X-ray diffraction

The XRD results revealed qualitative differences in the hydration process of the cementitious matrix due to the carbonation curing, corroborating to the TGA/DTG results. As can be seen in Fig. 7a, non-carbonated samples presented a higher intensity in the region of $2\theta = 18^\circ$ corresponding to the portlandite (calcium hydroxide) content for samples at 28 days of age. The carbonation process in the early stages of hydration resulted in the decrease of portlandite, as shown by the lower intensity of the characteristic peak (Fig. 7b).

3.2.4. Scanning electron microscopy

Micrographs observed in Figs. 8 and 9 were obtained by SEM in secondary electron mode of the fracture surfaces of non-carbonated and carbonated samples, respectively, which resulted from the mechanical test performed at 28 days (i.e. unaged composites).

Fig. 8a shows evidence of a large number of fibers pulled out from the matrix, which show their total length and absence of the cement hydration compounds on their surfaces due to the easy slipping of the fiber as a result of the poor bond fiber–matrix in a porous matrix (Fig. 8b).

Carbonated samples showed a reduced number of fibers pulled out from the matrix (Fig. 9a) due to the better fiber–matrix bonding and hydration compounds can be observed on the surface of the fiber (Fig. 9b). In this case, there is a balance between fiber adhesion and fiber strength and therefore a major number of fibers may rupture, instead of performing the complete frictional slip process. The micrographs also show a denser and compact matrix that improved the mechanical strength of the composites (Fig. 9a).

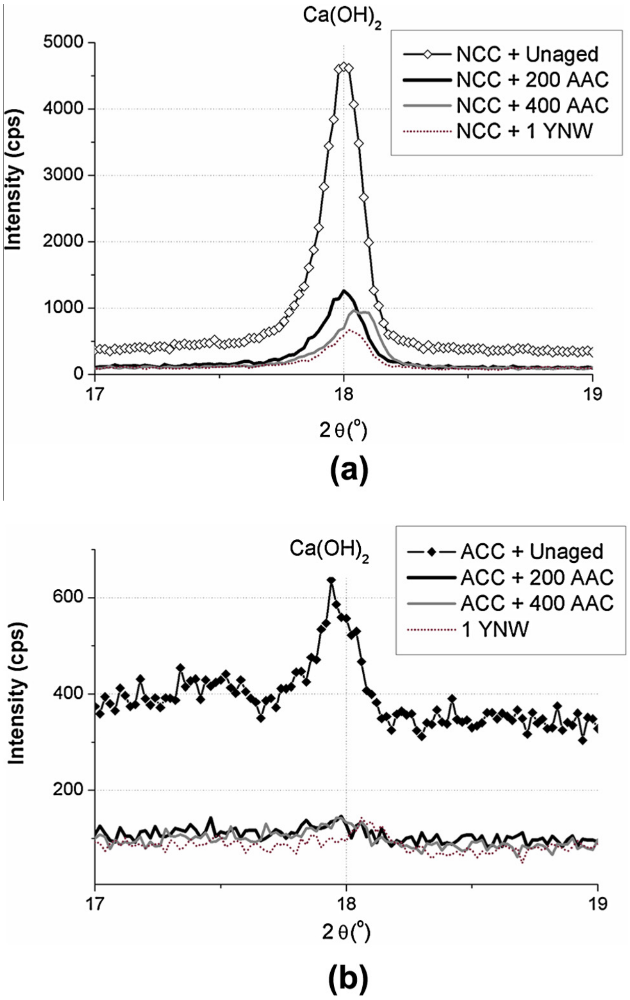

Fig. 7. XRD patterns of composites in the region of $2\theta = 18^\circ$, corresponding to the portlandite content: (a) non-carbonated; and (b) carbonated.

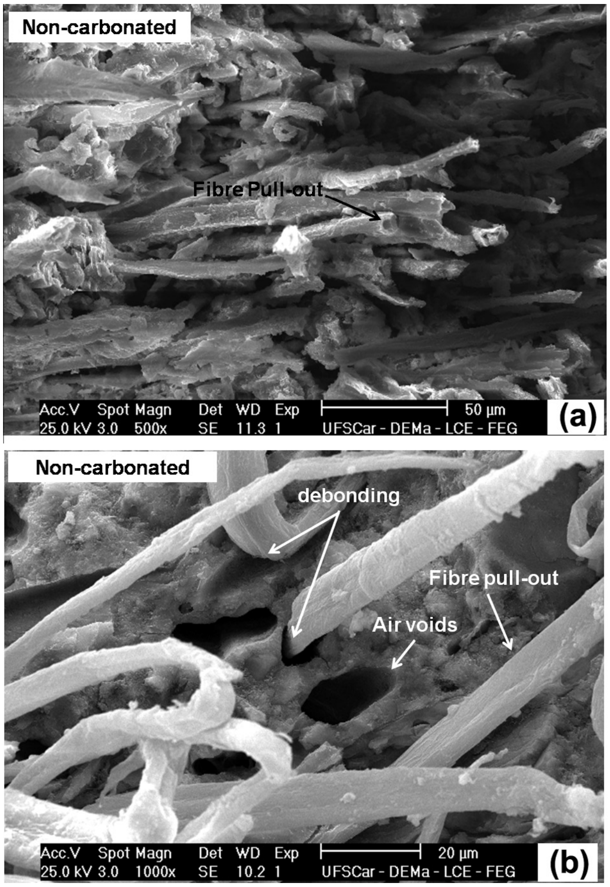

Fig. 8. Scanning electron micrographs of fracture surface of the unaged non-carbonated composite, after the mechanical test: (a) 500×; (b) 1000×.

Considering the cementitious matrix, the durability of the cement based materials can be successfully enhanced by reducing the permeability of liquids and gaseous elements from the external environment into the matrix [33]. It explains the mitigation of degradation of the carbonated composites as a result of the association of decreased porosity and increased bulk density with the higher precipitation of calcium carbonate, which is more stable and denser than calcium hydroxide. These results also contributed to the better fiber–matrix adhesion and the higher mechanical strength.

4. Conclusions

Accelerated carbonation after 2 days of controlled curing can be considered as a viable curing condition when looking for a durable eucalyptus cellulosic pulp reinforced cement based composite. Based on the results, mechanical properties were better for the composites subjected to accelerated carbonation at early stages of hydration (i.e. after 2 days of controlled curing) and these properties were maintained after accelerated and natural aging, indicating their improved durability. The decrease in the alkalinity of the cement matrix due to the lower $Ca(OH)_2$ content, lower porosity, smaller average pore diameter associated with the densification of the matrix by the higher precipitation of $CaCO_3$, which is a more

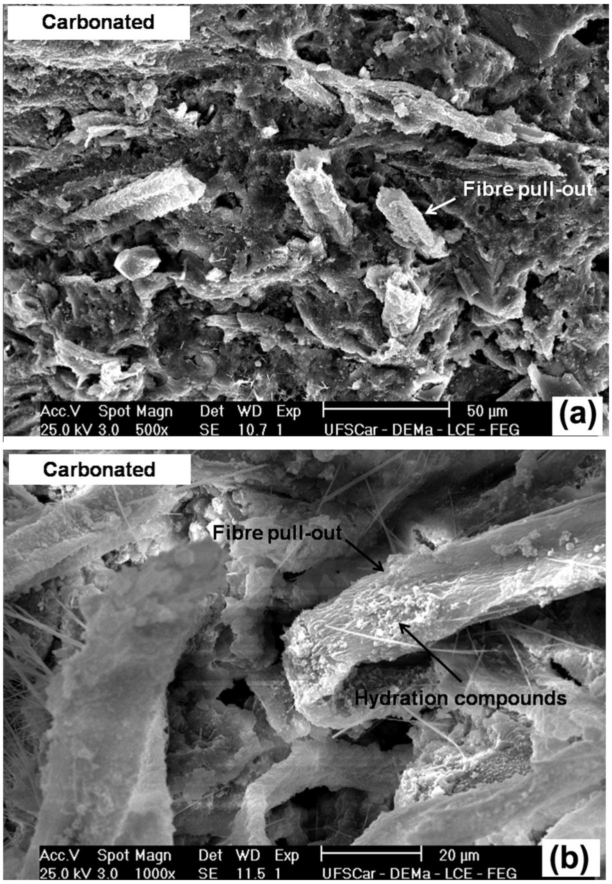

Fig. 9. Scanning electron micrographs of fracture surface of the unaged carbonated composite, after the mechanical test: (a) 500×; (b) 1000×.

stable and denser product than $Ca(OH)_2$, are the results of the carbonated curing. These results can explain the good fiber–matrix bonding, the improved mechanical properties and the mitigation of the composite degradation.

It is expected that the present results will encourage the use of vegetable pulps as an exclusive reinforcement in the fiber cement production and suggest the accelerated carbonation at early ages as a viable alternative for curing condition.

Acknowledgements

The authors would like to acknowledge financial support from the Fundação de Amparo à Pesquisa do Estado de São Paulo (Grants 2008/04769-9, 2009/10614-0, 2009/17293-5; 2010/16524-0), the Conselho Nacional de Desenvolvimento Científico e Tecnológico (processes: 472133/2009-8 and 305792/2009-1). The authors acknowledge Fibria Celulose S.A. as well as Infibra Ltda for providing Eucalyptus pulps and cementitious raw-materials respectively, and Mr. Zaqueu Freitas and Mr. Humberto Giroldo for their technical assistance.

References

[1] Ramakrishna T, Sundararajan T. Studies on the durability of natural fibres and the effect of corroded fibres on the strength of mortar. Cem Concr Compos 2005;27:575–82.

[2] Tonoli GHD, Santos SF, Savastano Jr H, Delvasto S, Mejía de Gutiérrez R, del M, et al. Effects of natural weathering on microstructure and mineral composition of cementitious roofing tiles reinforced with fique fiber. Cem Concr Compos 2011;33(2):225–32.

[3] Coutts RSP. A review of Australian research into natural fiber cement composites. Cem Concr Compos 2005;27:518–26.

[4] Bentur A, Akers SAS. The microstructure and ageing of cellulose fibre reinforced cement composites cured in a normal environment. Int J Cem Compos Lightweight Concr 1989;11(2):99–109.

[5] Mohr BJ, Nanko H, Kurtis KE. Durability of kraft pulp fiber–cement composites to wet/dry cycling. Cem Concr Compos 2005;27:435–48.

[6] Mohr BJ, Biernacki JJ, Kurtis KE. Supplementary cementitious materials for mitigating degradation of kraft pulp fiber–cement composites. Cem Concr Res 2007;37:1531–43.

[7] Tonoli GHD, Almeida AEFS, Pereira-da-Silva MA, Bassa A, Oyakawa D, Savastano Jr H. Surface properties of eucalyptus pulp fibers as reinforcement of cement-based composites. Holzforsch 2010;64:595–601.

[8] Tonoli GHD, Santos SF, Joaquim AP, Savastano Jr H. Effect of accelerated carbonation on cementitious roofing tiles reinforced with lignocellulosic fiber. Constr Build Mater 2010;24:193–201.

[9] Almeida AEFS, Tonoli GHD, Santos SF, Savastano Jr H. Accelerated carbonation in the early ages of cellulose pulps reinforced cement composites. Ambiente Construído 2010;10:233–46 [in Portuguese].

[10] Tolêdo Filho RD, Ghavami K, England GL, Scrivener K. Development of vegetable fiber – mortar composites of improved durability. Cem Concr Compos 2003;25:185–96.

[11] Fernández Bertos M, Muntean A, Simons SJR, Hills CD, Carey PJ. A review of accelerated carbonation technology in the treatment of cement-based materials and sequestration of CO_2. J Hazard Mater 2004;B112:193–205.

[12] Peter MA, Muntean A, Meier SA, Böhm M. Competition of several carbonation reactions in concrete: a parametric study. Cem Concr Res 2008;38:1385–93.

[13] Klemm WA, Berger RL. Accelerated curing of cementitious systems by carbon dioxide. Part I. Portland cement. Cem Concr Res 1972;2:567–76.

[14] Berger RL, Klemm WA. Accelerated curing of cementitious systems by carbon dioxide. Part II. Hydraulic calcium silicates and aluminates. Cem Concr Res 1972;2:647–52.

[15] Akers SAS, Studinka JB. Ageing behavior of cellulose fiber cement composites in natural weathering and accelerated tests. Int J Cem Compos Lightweight Concr 1989;11(2):93–7.

[16] Macvicar R, Matuana LM, Balatinecz JJ. Aging mechanism in cellulose fiber reinforced cement composites. Cem Concr Compos 1999;21(3):189–96.

[17] Tonoli GHD, Rodrigues Filho UP, Savastano Jr H, Bras J, Belgacem MN, Rocco Lahr FA. Cellulose modified fibers in cement based composites. Compos Part. A: Appl Sci Manuf 2009;40:2046–53.

[18] Tonoli GHD, Fuente E, Monte C, Savastano Jr H, Rocco Lahr FA, Blanco A. Effect of fibre morphology on flocculation of fibre–cement suspensions. Cem Concr Res 2009;39:1017–22.

[19] Brazilian Technical Standards Association (ABNT) NBR 5733. Portland cement of high initial strength: specification. Rio de Janeiro; 1983 [in Portuguese].

[20] Savastano Jr H, Warden PG, Coutts RSP. Brazilian waste fibers as reinforcement for cement-based composites. Cem Concr Compos 2000;22:379–84.

[21] Borges PHR, Costa JO, Milestone NB, Lynsdale CJ, Streatfield RE. Carbonation of CH and C–S–H in composite cement pastes containing high amounts of BFS. Cem Concr Res 2010;40:284–92.

[22] European Committee for Standardization. EN 494, Fiber–cement profiled sheets and fittings for roofing – Products specification and test methods BSI – British Standards Institution; 1994.

[23] Tonoli GHD, Savastano Jr H, Santos SF, Dias CMR, John VM, Lahr FAR. Hybrid reinforcement of sisal and polypropylene fibers in cement-based composites. J Mater Civ Eng 2011;23:177–87.

[24] American Society for Testing and Materials C 948-81. Test method for dry and wet bulk density, water absorption, and apparent porosity of thin sections of glass–fiber reinforced concrete. West Conshohocken, PA, USA; 1981.

[25] Diamond S. Mercury porosimetry: an inappropriate method for the measurement of pore size distributions in cement-based materials. Cem Concr Res 2000;30:1517–25.

[26] Dweck J, Buchler PM, Coelho ACV, Cartledge FK. Hydration of a Portland cement blended with calcium carbonate. Thermochim Acta 2000;346:105–13.

[27] Fordham CJ, Smalley IJ. A simple thermogravimetric study of hydrated cement. Cem Concr Res 1985;15:141–4.

[28] Vedalakshmi R, Sundara Raj A, Srinivasan S, Ganesh Babu K. Quantification of hydrated cement products of blended cements in low and medium strength concrete using TGA and DTA technique. Thermochim Acta 2003;407:249–60.

[29] Claramunt J, Ardanuy M, García-Hortal JA. Effect of drying and rewetting cycles on the structure and physicochemical characteristics of softwood fibres for reinforcement of cementitious composites. Carbohydr Polym 2010;79:200–5.

[30] Cordero T, Rodríguez-Maroto JM, Rodríguez-Mirasol J, Rodríguez JJ. On the kinetics of thermal decomposition of wood and wood components. Thermochim Acta 1990;164:135–44.

[31] Prins J, Ptasinski KJ, Janssen FJJG. Torrefaction of wood. Part 1. Weight loss kinetics. J Anal Appl Pyrolysis 2006;77:28–34.

[32] Soroushian P, Wonb J, Hassan M. Durability characteristics of CO_2-cured cellulose fiber reinforced cement composites. Constr Build Mater 2012;34:44–53.

[33] Mehta PK, Monteiro PJM. Concrete: microstructure, properties, and materials. New York: McGraw Hill; 2006.